Eur. Phys. J. A **20**, 405–411 (2004)
DOI 10.1140/epja/i2003-10171-6

THE EUROPEAN PHYSICAL JOURNAL A

The N = Z nucleus ^{76}Sr: Gamow-Teller strength and nuclear deformation

Ph. Dessagne[1,a], M.J.G. Borge[2], J. Giovinazzo[1,b], A. Huck[1], A. Jokinen[3], A. Knipper[1], C. Longour[1], G. Marguier[4], M. Ramdhane[3,c], V. Rauch[1], O. Tengblad[2,3], G. Walter[1], Ch. Miehé[1], and the ISOLDE Collaboration[3]

[1] Institut de Recherches Subatomiques, UMR 7500 CNRS-IN2P3 et Université Louis Pasteur, 23 rue du Loess, B.P. 28, F-67037 Strasbourg Cedex 2, France
[2] Instituto de Estructura de la Materia, CSIC, Serrano 113bis, E-28006 Madrid, Spain
[3] ISOLDE, Division EP, CERN, CH-1211 Geneva, Switzerland
[4] Institut de Physique Nucléaire, Université Claude Bernard-Lyon I, F-69622 Villeurbanne Cedex, France

Received: 26 June 2003 / Revised version: 5 November 2003 /
Published online: 18 June 2004 –
Communicated by J. Äystö

Abstract. Challenged by recent theoretical work, a study of the β^+-EC decay of the $N = Z$ even-even nucleus ^{76}Sr has been undertaken in order to assign the parent ground-state deformation. In this study 13 levels with $J^\pi = 1^+$ have been located in ^{76}Rb. The beta-delayed proton emission has been observed for the first time in an $N = Z$ even-even nucleus. The βp branching ratio has been determined to be $(3.4 \pm 0.8) \cdot 10^{-5}$. The ^{76}Sr half-life has been remeasured and a more precise value of 7.89 ± 0.07 s has been obtained. On the basis of the comparison of measured Gamow-Teller strength with calculated strength distributions for both oblate and prolate deformation, it is concluded that the ^{76}Sr has strong prolate deformation in the ground state.

PACS. 21.10.Hw Spin, parity, and isobaric spin – 23.20.Lv γ transitions and level energies – 23.40.Hc Relation with nuclear matrix elements and nuclear structure – 27.50.+e $59 \leq A \leq 89$

1 Introduction

Nuclear deformation is one of the keys to nuclear structure, but it is not always straightforward to obtain it as illustrated by sometimes conflicting calculations of the ground-state shapes [1–3] resulting from different theoretical approaches. In this frame, nuclei located along the $N = Z$ line are of special interest as transitions from spherical, oblate, prolate and again spherical shapes are expected to occur when going from $A = 40$ to $A = 100$. In this respect a strong sudden shape transition between oblate and prolate deformation is predicted to happen between $N = Z = 36$ and $N = Z = 38$ [4,5]. From in-beam experimental work carried out by W. Gelletly and coworkers [6] with fusion-evaporation reaction γ-ray spectroscopy, the lowest 2^+ states in the even-even isotopes from $A = 64$ to $A = 84$ have been located, and the first indication for changes in ground-state deformation in the series has been obtained. Nevertheless the oblate or prolate character of the deformation could not be inferred from these measurements. From the pioneering calculations performed by I. Hamamoto *et al.*, on the Gamow-Teller (GT) decay for the neutron-deficient nuclei along the $N = Z$ line, major differences in the GT-strength were found to exist for the cases of oblate and prolate deformation. Above mass $A = 60$, the GT Giant Resonance (GTGR) is expected to be located below the mother ground state and the main part of the strength should become accessible to the β^+-EC decay process [7]. In addition, the GT-strength distribution should provide valuable information on nuclear deformation in the N close to Z neutron-deficient mass region [8]. As a result of the work carried out by these authors in the Hartree-Fock and Tamm-Dancoff approach, the decays predicted for various deformations (oblate and prolate minima, spherical constraint form) exhibit clear differences in terms of both integrated GT-strength and GT-strength distributions. Developments in this field, carried out by P. Sarriguren *et al.*, corroborates these predictions [9,10]. The location of the GTGR and the distribution of the GT-strength are both sensitive to the sign of the deformation.

[a] e-mail: philippe.dessagne@ires.in2p3.fr
[b] *Present address*: Centre d' Etudes Nucléaires de Bordeaux-Gradignan, Le Haut Vigneau, F-33175 Gradignan Cedex, France.
[c] *Present address*: University Mentouri, 25000 Constantine, Algeria.

Stimulated by these predictions, we have undertaken the study of the radioactive decay of the even-even nuclei available at the CERN ISOLDE facility. We report here on new experimental results obtained in the analysis of the β^+-EC decay of ^{76}Sr, nucleus on which little was known from previous investigations [11,12]. Beta-delayed particle emission is energetically open in this decay for both proton and α channels. In addition to the beta gamma decay measurements, the detection of delayed particle emission allows weak GT branches to be detected in the upper part of the $Q_{\rm EC}$ window. The GT-strength will be discussed in the frame of the currently available theoretical estimates in order to extract information on the deformation of the ground state of the parent nucleus.

2 Experimental procedure

The ^{76}Sr isotope has been produced at the CERN ISOLDE/PSB facility by fragmentation of a 48 g/cm^2 niobium target induced by the pulsed 1 GeV proton beam of the Proton Synchrotron Booster of 2 μA mean intensity. In order to achieve chemical selectivity a low partial pressure of CF_4 is introduced in the ion source and the isotope of interest is extracted as an SrF^+ molecular combination [13,14]. Currently obtained yields range from 2 to 7.10^3 at/s. The mass-selected beam is steered towards a tape transport system serving two independent counting stations. The first one, surrounding the beam collection point, was devoted to $4\pi\beta$, $4\pi\beta\cdot\gamma$, $4\pi\beta\cdot\gamma\cdot\gamma$ direct, multispectra and coincidence measurements. The collection point was surrounded by a plastic scintillator of 80% efficiency for the detection of the β-particles and two HPGe counters of 80% and 70% efficiency, each covering 5% of 4π, were mounted facing the collected sources. The second one, the measurement point, to which the radioactive source is moved synchronously, is equipped to detect delayed particles emission and the related X- and γ-rays. The particle detection is ensured by a C_4H_{10} gas-silicon telescope which allows heavy charged particles (protons and alpha) to be observed in the presence of a high background coming from the interaction of positrons with the detector. It covered a solid angle of 10.1(5)% of 4π. Conventional α sources and the conversion electrons of a ^{207}Bi source were used for calibration. The ΔE counter response is parametrized according to an energy loss computer code. A mean energy resolution of 60 keV FWHM was obtained for the delayed particles. At this measuring point an Si(Li) low-energy γ-ray counter was mounted allowing the detection of photons with an energy up to 100 keV and covering a solid angle of 15% of 4π. A HPGe detector devoted to the observation of γ in the 70–4500 keV energy range was placed at this upper station covering 5% of 4π. The measurements are performed in duty cycles (collection, counting and source displacement) managed by a microcomputer. This allows flexible and independent data taking for the two stations, synchronized with the PS Booster supercycle. The contribution of the background generated by the proton burst impinging on the target is suppressed by inhibiting the acquisition during 20 ms after each proton burst.

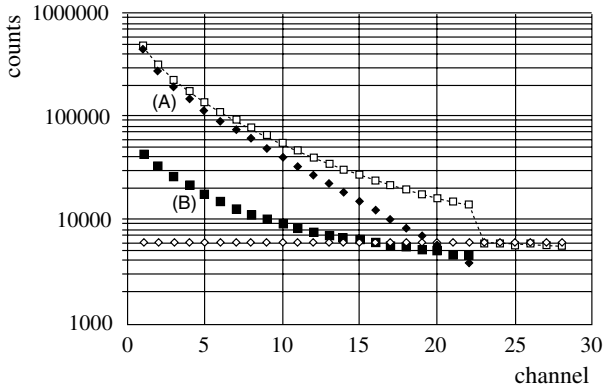

Fig. 1. Multiscaling obtained for the β-particles emitted in the decay of ^{76}Sr (10.24 s/ch). The empty squares are the experimental points. The constant background is given by empty diamonds. The contributions from ^{76}Sr and ^{76}Rb (curve (A)) are displayed as full diamonds and those from ^{79}Y and ^{79}Sr (curve (B)) are indicated by full squares.

3 Experimental results

3.1 The ^{76}Sr half-life

High-statistics β-decay measurements have been performed with the help of the $4\pi\beta$ scintillation counter surrounding the tape at the collection point. The activity of 28 sources, with 14 seconds collection time, has been registered as a function of time using a time digital converter encoded on 4096 channels of 80 ms each. After a 240 s counting period the sources were moved to a shielded area, leaving 70 s to measure the background activity (see fig. 1). The analysis of the binned data is performed by a multiparametric least-squares fit method, in which the parent and daughter half-life are free parameters. The parasitic beam of $^{79}YO^+$ originating from the oxygen partial pressure in the target is also taken into account, and the amount of contamination as well as the corresponding half-life are free parameters of the fit too. A precise value is obtained for the ^{76}Sr half-life $T_{1/2} = 7.89\pm0.07$ s (fig. 1), 10% shorter than the previously reported one [11], shorter also than the values inferred from the different mass formulae by M. Hirsch *et al.* [15], but pretty close to the estimate of G.T. Biehle *et al.* based on the random phase approximation [16]. From our measurements a new value is also inferred for the half-life of ^{76}Rb, $T_{1/2} = 35.40(12)$ s which is slightly shorter and more precise than the previous determinations [17].

3.2 Bound levels in ^{76}Rb

The γ-rays attributed to the decay of ^{76}Sr have been selected on the basis of multispectra analysis and coincidence measurements. They are listed in table 1, with their

Table 1. Gamma transitions in the β-decay of ^{76}Sr, those with * are not placed in the decay scheme. For absolute intensity per 100 decays multiply by 0.495. Placement based in energetics.

E (keV)	I + IC	E_i (keV)	E_f (keV)
39.0 ± 0.5	90.95 ± 17.11	516.	477.
101.4 ± 0.5	66.59 ± 10.94	101.	0.
145.2 ± 0.5	7.09 ± 1.13	247.	101.
192.4 ± 0.5	2.72 ± 0.51	708.	516.
231.0 ± 0.5	7.67 ± 1.37	477.	247.
246.6 ± 0.5	2.27 ± 0.29	247.	0.
375.2 ± 0.5	29.82 ± 3.62	477.	101.
414.4 ± 0.5	14.97 ± 1.48	516.	101.
453.0 ± 0.5	2.35 ± 0.23	969.	516.
466.9 ± 0.5	2.66 ± 0.29	983.	516.
476.8 ± 0.5	100.	477.	0.
494.0 ± 0.5*	5.83 ± 1.06	–	–
506.1 ± 0.5	11.68 ± 1.35	983.	477.
515.8 ± 0.5	6.80 ± 0.81	516.	0.
550.1 ± 0.5	4.57 ± 0.54	1533.	983.
563.7 ± 0.5*	1.3 ± 0.2	–	–
580.8 ± 0.5	6.45 ± 0.79	1289.	708.
608.0 ± 0.5	0.81 ± 0.12	708.	101.
657.3 ± 0.5	0.67 ± 0.11	1640.	983.
679.7 ± 0.5	1.01 ± 0.16	2091.	1413.
707.8 ± 0.5	1.91 ± 0.41	708.	0.
726.8 ± 0.5	0.98 ± 0.15	2140.	1413.
812.8 ± 0.5	2.51 ± 0.25	1289.	477.
882.4 ± 0.5	10.82 ± 1.15	983.	101.
935.9 ± 0.5	1.76 ± 0.20	1413.	477.
982.9 ± 0.5	21.97 ± 2.52	983.	0.
1124.0 ± 0.5	0.95 ± 0.11	1640.	516.
1171.2 ± 0.5	2.69 ± 0.26	2140.	969.
1187.0 ± 0.5	0.53 ± 0.07	1289.	101.
1432.1 ± 0.5	1.19 ± 0.14	1948.	516.
1471.3 ± 0.5	0.64 ± 0.08	1948.	477.
1546.0 ± 0.5	2.72 ± 0.33	2062.	516.
1568.3 ± 0.5*	0.56 ± 0.12	–	–
1584.9 ± 0.5	1.19 ± 0.12	2062.	477.
1592.7 ± 0.5	0.73 ± 0.07	2882.	1289.
1612.5 ± 0.5	0.77 ± 0.09	2091.	477.
1624.4 ± 0.5	2.32 ± 0.22	2140.	516.
1657.0 ± 0.5	0.56 ± 0.07	2173.	516.
1695.7 ± 0.5	0.97 ± 0.10	2173.	477.
1805.0 ± 0.5	2.57 ± 0.25	2282.	477.
2039.0 ± 0.5	0.66 ± 0.08	2140.	101.
2140.5 ± 0.5	0.34 ± 0.05	2140.	0.
2172.5 ± 0.5	0.41 ± 0.06	2173.	0.
2248.9 ± 0.5*	0.72 ± 0.16	–	–
2499.9 ± 0.5*	0.27 ± 0.07	–	–
2684.5 ± 0.5*	0.21 ± 0.05	–	–
2719.1 ± 0.5*	0.74 ± 0.17	–	–
2934.6 ± 0.5*	0.77 ± 0.18	–	–

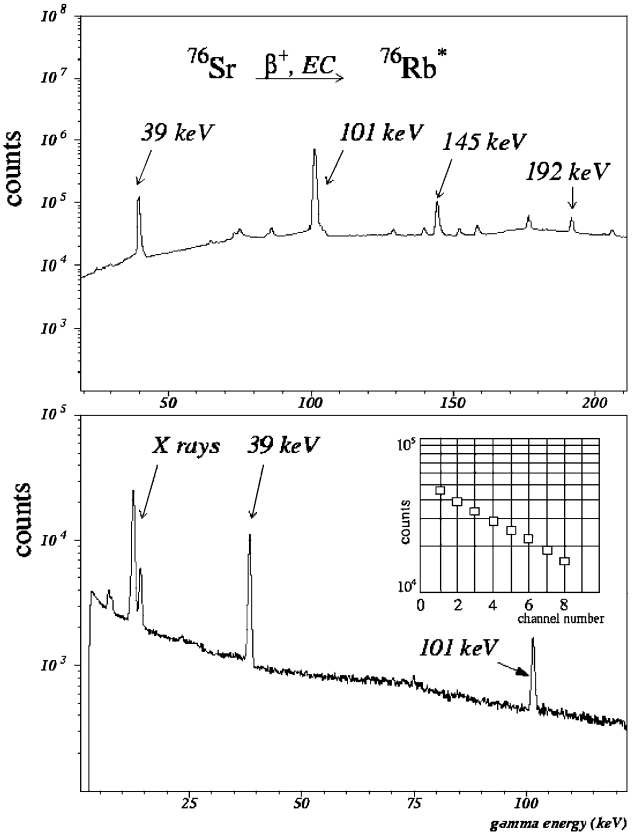

Fig. 2. Gamma-ray energy distribution obtained in the HPGe (top) and X-ray (bottom) detectors. In the inset the decay curve obtained for the 39 keV gamma line (1.7 s/ch) is shown.

relative intensity after correction for internal conversion. Among them, forty could be built into a coherent decay scheme. According to the spin-parity of the involved levels, for the low-energy gamma transitions at 39, 101, 145, 192 and 246.6 keV the $M1$ multipolarity has been considered. For the transition at 230 keV the $M2$ character has been taken into account. Among the new lines reported, we observed the 39 keV line which was out of the range of the energy spectrum registered in ref. [12]. This line is assigned to ^{76}Sr on the basis of its half-life as shown in the inset of fig. 2. Its location in the decay scheme is unambiguously established from our coincidence data. Up to now 13 unreported levels have been located up to 2882 keV excitation energy (see fig. 3). Corresponding γ branching ratios are indicated in table 2.

The β^+-EC branching ratios derived from the gamma inbalance are reported in table 3 together with the corresponding log ft values and the B(GT) values given by B(GT) = 4135 s · (ft)$^{-1}$. The β ground-state transition has been evaluated at the measurement point, where no accidental build-up of activity on a collimator can occur. The daughter activity results then only from the radioactive filiation laws and the collection-measurement time sequences. In the evaluation, the time structure of the proton beam delivered by the PS Booster and the release

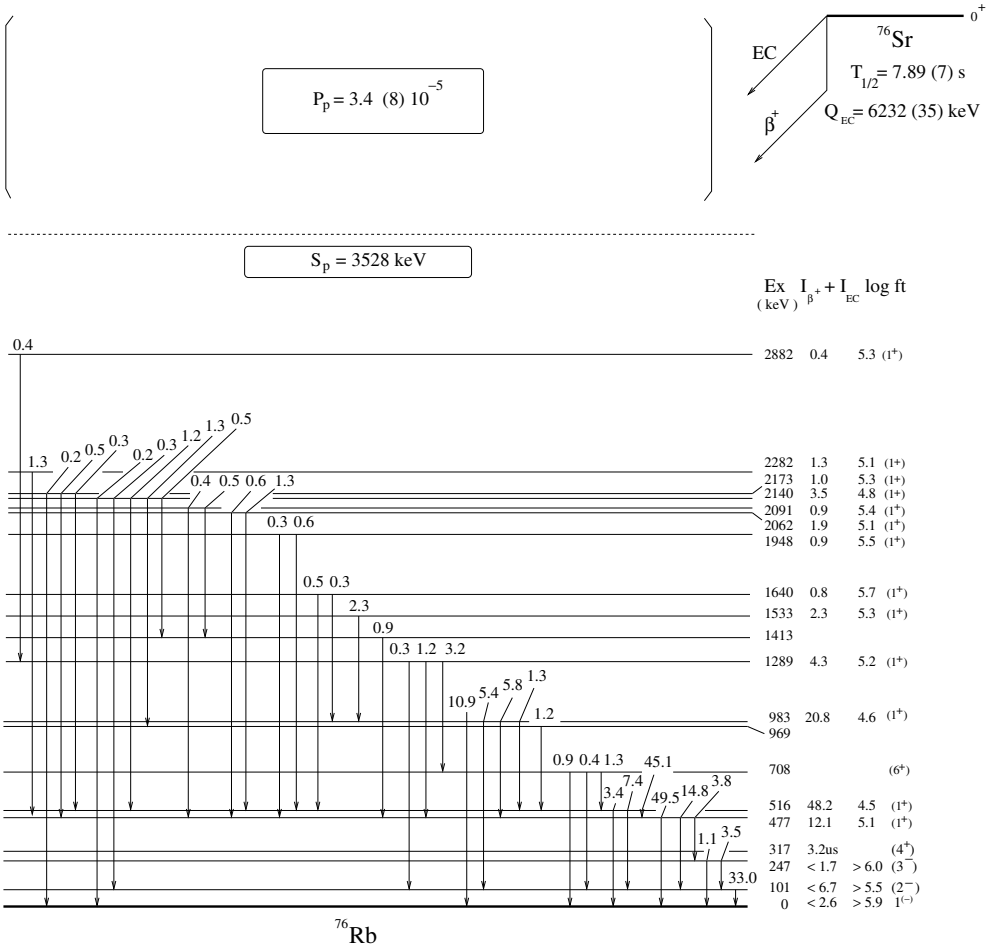

Fig. 3. Proposed decay scheme for ^{76}Sr. The intensity per 100 decays is given for each gamma transition.

time of the target are taken into account [18]. From various comparisons of the intensity of the prominent γ lines of our decay scheme with the main γ transitions (424, 797, 1680, 2571 keV) in the ^{76}Rb decay [12], an upper limit of 2.6% is obtained as weighted average for the direct β-feeding to the ^{76}Rb ground state. This value is in favour of a negative-parity assignment of this state for which $J^\pi = 1^{(-)}$ has been proposed [19,20].

A spin and parity 1^+ is assigned to 13 states in ^{76}Rb (see table 2) on the basis of the allowed character of their β-feeding from the 0^+ ground state of ^{76}Sr.

3.3 The delayed particle emission

From the energy diagram of the ^{76}Sr decay, a narrow energy range is open to delayed proton (2702 ± 39 keV) and alpha (2508 ± 262 keV) emission. These values have been calculated using the proton separation energy in ^{76}Rb ($S_\mathrm{p} = 3528(17)$ keV) and Q_α taken from [21] and the new mass value of ^{76}Sr determined by the Penning trap method at CERN ISOLDE [22]. Then the considered Q_EC value of the ^{76}Sr decay is 6232 ± 35 keV. The use of a gas-silicon telescope allows to distinguish between the three kinds of charged particles, the positrons, the protons and alphas, emitted in the radioactive decay. Such counter has been used in our previous work on the decay of ^{72}Kr [23]. In the registered ΔE-E spectrum, no α-particles are present, as expected from the Coulomb barrier effect, but delayed protons are observed. β-delayed protons from the ^{77}Sr decay were studied with the same setup during the same experiment with the purpose of internal calibration. The resulting ΔE-E bidimensional spectrum is shown in the inset of fig. 4. Separation between positrons and protons is clearly observed and the latter are delimited by a polygon. The same polygon has been used for the study of β-delayed protons in the neighbour isotope ^{76}Sr. In order to obtain the P_p value, the number of delayed protons from the ^{76}Sr decay is compared to the intensities of the 375, 414, 477, 882 and 983 keV gamma lines in ^{76}Rb. The weighted average of these evaluations gives a P_p value of $(3.4 \pm 0.8) \cdot 10^{-5}$. The reconstructed proton energy distribution, obtained after suitable calibration of the telescope, extends from 1.4 MeV up to 2.6 MeV (see fig. 5) covering almost the full energy window available. The upper limit is quite close to the determined Q_EC value of the

Table 2. Energies, spins and parities of adopted levels in ^{76}Rb, de-exciting gamma transitions and gamma-ray branching ratios.

E_x (keV)	J^π	E_γ (keV)	$I_{\gamma+\mathrm{IC}}$ (%)
101.4 ± 0.5	(2^-)	101.4	100.
246.6 ± 0.4	(3^-)	145.2	75.8 ± 3.8
		246.6	24.2 ± 3.8
477.0 ± 0.3	1^+	231.0	5.6 ± 1.1
		375.2	21.7 ± 2.7
		476.8	72.7 ± 3.0
515.9 ± 0.3	1^+	39.0	80.7 ± 3.2
		414.4	13.3 ± 2.3
		515.8	6.0 ± 1.1
708.4 ± 0.3	–	192.4	50.0 ± 6.1
		608.0	14.8 ± 2.6
		707.8	35.2 ± 5.9
969.0 ± 0.4	–	453.0	100.
983.1 ± 0.2	1^+	466.9	5.7 ± 0.7
		506.1	24.8 ± 2.6
		882.4	22.9 ± 2.3
		982.9	46.6 ± 3.4
1289.3 ± 0.2	1^+	580.8	67.9 ± 3.3
		812.8	26.5 ± 3.0
		1187.0	5.6 ± 0.8
1413.0 ± 0.4	–	935.9	100.
1533.2 ± 0.3	1^+	550.1	100.
1640.2 ± 0.2	1^+	657.3	41.3 ± 4.7
		1124.0	58.7 ± 4.7
1948.2 ± 0.3	1^+	1432.1	65.2 ± 4.0
		1471.3	34.8 ± 4.0
2062.0 ± 0.3	1^+	1546.0	69.6 ± 3.3
		1584.9	30.4 ± 3.3
2090.9 ± 1.1	1^+	679.7	56.7 ± 4.7
		1612.5	43.3 ± 4.7
2140.3 ± 0.2	1^+	726.8	14.0 ± 2.0
		1171.2	38.5 ± 2.8
		1624.4	33.2 ± 2.6
		2039.0	9.5 ± 1.1
		2140.5	4.9 ± 0.7
2172.8 ± 0.2	1^+	1657.0	28.9 ± 3.1
		1695.7	50.0 ± 3.5
		2172.5	21.1 ± 2.6
2282.1 ± 0.4	1^+	1805.0	100.
2882.1 ± 0.3	1^+	1592.7	100.

systematics [21]. It has to be mentionned that delayed proton emission is observed for the first time in an even-even $N = Z$ nucleus.

Table 3. Beta branching ratios, $\log(f_0 t)$ and B(GT) values for the feeding to the bound levels in ^{76}Rb.

E_x (keV)	%beta	$\log(f_0 t)$	B(GT)10^{-5}
0.0	< 2.6	> 5.9	$> 0.$
101.4	< 6.75	> 5.5	$< 1296.$
246.6	< 1.73	> 6.0	$< 379.$
477.0	12.1 ± 10.3	5.1 (−0.8 +0.3)	$3300. \pm 2652.$
515.9	48.2 ± 8.5	4.5 (−0.1 +0.1)	$13631. \pm 2619.$
708.4	< 0.01	> 8.0	$< 4.$
969.0	< 0.005	> 8.2	$< 2.$
983.1	20.8 ± 1.6	4.6 (−0.1 +0.1)	$9455. \pm 973.$
1289.3	4.34 ± 0.41	5.2 (−0.1 +0.1)	$2776. \pm 343.$
1413.0	< 0.03	> 7.3	$< 22.$
1533.2	2.26 ± 0.27	5.3 (−0.1 +0.1)	$1928. \pm 281.$
1640.2	0.80 ± 0.07	5.7 (−0.1 +0.1)	$780. \pm 96.$
1948.2	0.90 ± 0.08	5.5 (−0.1 +0.1)	$1309. \pm 160.$
2062.0	1.94 ± 0.17	5.1 (−0.1 +0.1)	$3276. \pm 408.$
2090.9	0.88 ± 0.09	5.4 (−0.1 +0.1)	$1552. \pm 210.$
2140.3	3.47 ± 0.19	4.8 (−0.0 +0.0)	$6551. \pm 627.$
2172.8	0.96 ± 0.07	5.3 (−0.1 +0.1)	$1904. \pm 207.$
2282.1	1.27 ± 0.13	5.1 (−0.1 +0.1)	$2946. \pm 400.$
2882.1	0.36 ± 0.04	5.3 (−0.1 +0.1)	$2215. \pm 326.$

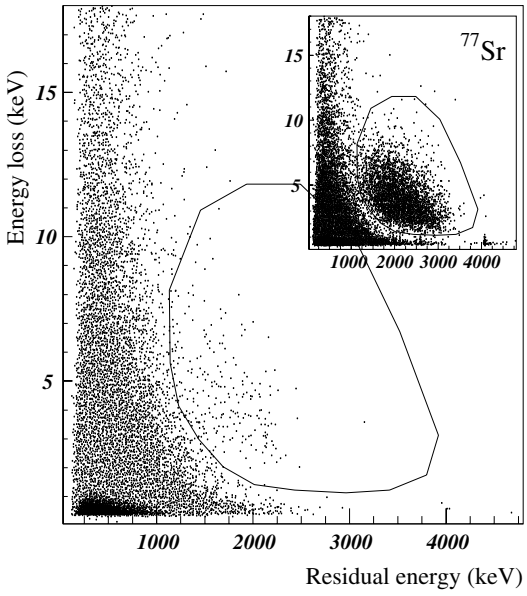

Fig. 4. Bidimensional distribution for beta-delayed particles from ^{76}Sr decay. The inset shows the β-delayed protons from the ^{77}Sr decay used for internal calibration. The polygons used to select the protons are identical.

4 Gamow-Teller strength and nuclear deformation

The ^{76}Sr isotope has revealed to be the most deformed $N = Z$ even-even nucleus observed in the in-beam fusion-evaporation reaction studies [6]. The excitation energy of the first 2^+ excited state $E_x = 261$ keV yields a deformation parameter $|\varepsilon_2| = 0.45$ according to Grodzins' formula, but the oblate or prolate character cannot be inferred from this result.

According to the theoretical estimates by I. Hamamoto and X.Z. Zhang [7] performed in the frame of a quasiparticle Tamm-Dancoff approximation based on Skyrme-type deformed Hartree-Foch calculations, a noticeable difference in the Gamow-Teller β^+-EC decay matrix elements is expected between an oblate and prolate deformation of the parent nucleus for the $N = Z$ even-even nuclei with $A = 72$–80, especially for ^{76}Sr. On this basis, a comparison of our experimental results with the predictions related to the deformation of the ground state of

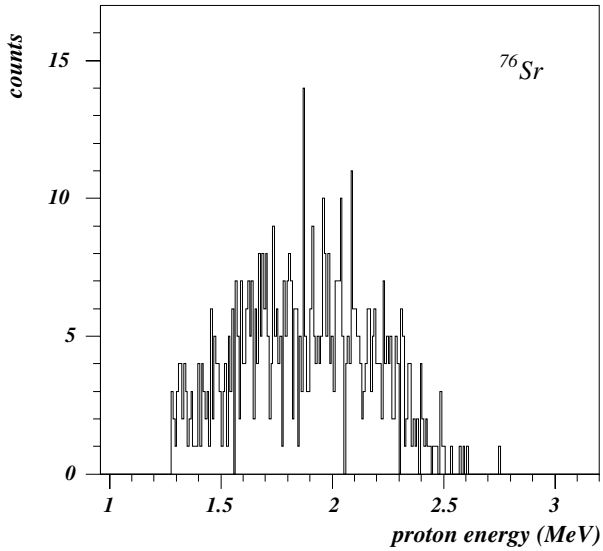

Fig. 5. Proton energy distribution.

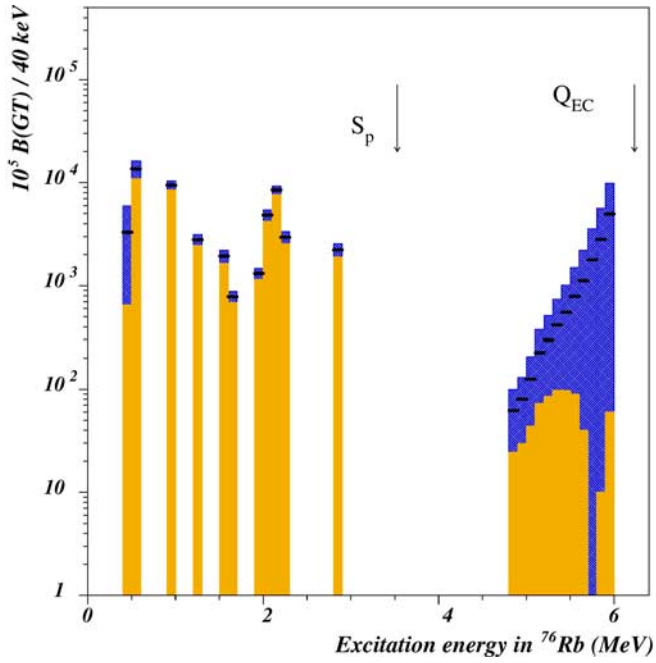

Fig. 6. Gamow-Teller strength distribution observed in ^{76}Sr decay.

^{76}Sr has been done intending to obtain a signature of the nuclear shape.

The Gamow-Teller strength distribution deduced from our data is reported in fig. 6. At high excitation energy the large error bars on the quoted values come from the poor statistics in the proton channel. Due to the spread of the γ-strength over numerous open channels and the drop of the photopeak efficiency with increasing γ-ray energy, the radiative de-excitation escapes our observation above the proton separation energy. The upper part of the B(GT) distribution reflects therefore only the delayed proton channel contribution to the β-EC strength. No γ-proton coincidence data were observed due to the weak delayed proton branch. Only proton emission to the ^{75}Kr ground state has therefore been considered to evaluate the experimental B(GT) values above the proton separation energy.

Table 4. Comparison between experimental and predicted Gamow-Teller strengths for the ^{76}Sr decay.

Gamow-Teller strengths	Experiment	Theory [7]/[10][(b)]	
		Oblate	Prolate
ΣB(GT) unbound states	0.13 ± 0.06[(a)] 6.5 ± 3.0	0.4/1.6	4.5/5.25
ΣB(GT) bound states	0.52 ± 0.04	2.9/2.3	1.4/1.55

([a]) This part of the β-strength comes only from β-delayed proton emission (estimated to be only 2% of the ΣB(GT) in the Q_{EC}-S_p window).
([b]) Theoretical values do not include the quenching factor.

The Gamow-Teller strength expected from the theoretical estimates of I. Hamamoto *et al.*, [7] and P. Sarriguren *et al.*, [10] for the oblate and prolate cases over the energy window in ^{76}Rb from 0 to S_p (bound states) and the Q_{EC}-S_p (unbound states) are quoted in table 4. These mean-field calculations with residual interaction treated in QTDA [7] and QRPA [10] give similar ΣB(GT) values making meaningful the comparison with the values deduced from our experimental data. This makes ^{76}Sr an optimum case to deduce the sign of the deformation of the ground state from the GT-strength distribution.

The overall β-strength is obviously smaller than the calculated one, as is expected from the missed γ-strength due to our instrumental limitation. For the bound states, for which the radiative decay is known to be well detected, the corresponding β-strength is compatible with the expected value in the prolate case when a quenching factor of 0.6 for both calculations, [7] and [10] is taken into account. The work performed by our group on the statistical analysis of the delayed proton emission of the $T_Z = 1/2$ precursors [24] has allowed us to make a realistic evaluation of the unobserved gamma $E1$ intensity of the unbound levels. The decay of the ^{76}Sr ground state has been simulated considering J.C. Hardy *et al.* parametrization [25]. The level density has been estimated in the Back shifted Fermi Gas Model with a level density parameter $a = 11\,\mathrm{MeV}^{-1}$. As result of our evaluation the delayed proton channel has been estimated to be only 2% of the ΣB(GT) in the Q_{EC}-S_p window. The experimental ΣB(GT) value to unbound levels corrected for gamma-decay lies in the vicinity of the predicted strength for the prolate deformation (table 4). This result is in agreement with what is expected from the deformed Hatree-Fock calculations in terms of absolute minimum of the total potential energy curve.

5 Summary and concluding remarks

The detailed analysis of the Gamow-Teller decay of the even-even $N = Z = 38$ shell gap strontium isotope has

revealed several interesting features in both the parent and daughter nucleus. Thirteen up-to-now unreported levels have been located in ^{76}Rb. Thirteen have been assigned to have spin and parity 1^+ on the basis of their feeding by allowed Gamow-Teller transitions. The comparison between the experimentally determined ΣB(GT) and the theoretical calculations of [7] and [10] in the region of bound states allows to conclude that the deformation of the ^{76}Sr ground state is prolate. The deformation parameter of [10] for the prolate deformation is $\beta = 0.42$, consistent with the value deduced from the determination of the excitation energy of the 2^+ level in ^{76}Sr [6]. The study of the delayed proton emission combined with statistical calculations to estimate the missing gamma-strength permit to deduce a ΣB(GT) value for this unbound region that corroborates the sign of the ground-state deformation for ^{76}Sr.

The authors are indebted to I. Hamamoto for her early calculations that supported the experimental proposal at ISOLDE (CERN). They would also like to thank R.A. Molina, E. Moya de Guerra, A. Poves, J. Retamosa, P. Sarriguren and A. Zuker for very fruitful discussions. This work was partially supported by the Spanish Agency CICYT under contract Nos. AEN96-1679 and AEN99-1046-C02-01, and by the French and Spanish Agreement IN2P3-CICYT.

References

1. P. Bonche *et al.*, Nucl. Phys. A **443**, 39 (1989).
2. A. Petrovici *et al.*, Nucl. Phys. A **665**, 333 (2000).
3. W. Nazarewicz *et al.*, Nucl. Phys. A **435**, 397 (1985).
4. Y. Aboussir *et al.*, Nucl. Data Tables **61**, 127 (1995).
5. P. Moller *et al.*, Nucl. Data Tables **59**, 185 (1995).
6. W. Gelletly *et al.*, Phys. Lett. B **253**, 287 (1991).
7. I. Hamamoto, X.Z. Zhang, Z. Phys. A **353**, 145 (1995).
8. F. Frisk *et al.*, Phys. Rev. C **52**, 5 (1995).
9. P. Sarriguren *et al.*, Nucl. Phys. A **658**, 13 (1999).
10. P. Sarriguren *et al.*, Nucl. Phys. A **691**, 631 (2001).
11. H. Grawe *et al.*, Z. Phys. A **341**, 247 (1992).
12. P.R. Adzic *et al.*, Phys. Rev. C **48**, 2598 (1993).
13. P. Hoff *et al.*, Nucl. Instrum. Methods **172**, 413 (1980).
14. C.F. Liang *et al.*, Z. Phys. A **309**, 185 (1982).
15. M. Hirsch *et al.*, At. Data Nucl. Data Tables **53**, 165 (1993).
16. G.T. Biehle, P. Vogel, Phys. Rev. C **46**, 1555 (1992).
17. B. Singh *et al.*, Nucl. Data Sheets **42**, 233 (1984).
18. J. Lettry, private communication.
19. D.M. Moltz *et al.*, Phys. Lett. B **113**, 16 (1982).
20. D.M. Moltz *et al.*, Nucl. Phys. A **427**, 317 (1984).
21. G. Audi *et al.*, Nucl. Phys. A **624**, 1 (1997).
22. F. Herfurth *et al.*, to be published in Nucl. Phys. A.
23. I. Piqueras *et al.*, Eur. Phys. J. A **16**, 313 (2003).
24. J. Giovinazzo *et al.*, Nucl. Phys. A **674**, 394 (2000).
25. J.C. Hardy *et al.*, Phys. Lett. B **109**, 242 (1982).